



Published in final edited form as:

Toxicol Appl Pharmacol. 2016 July 15; 303: 65–78. doi:10.1016/j.taap.2016.04.016.

Resveratrol protects the ovary against chromium-toxicity by enhancing endogenous antioxidant enzymes and inhibiting metabolic clearance of estradiol

Sakhila K. Banu^{*}, Jone A. Stanley, Kirthiram K. Sivakumar, Joe A. Arosh, and Robert C. Burghardt

Department of Veterinary Integrative Biosciences, College of Veterinary Medicine and Biomedical Sciences, Texas A&M University, College Station, TX 77843, USA

Abstract

Resveratrol (RVT), a polyphenolic component in grapes and red wine, has been known for its cytoprotective actions against several diseases. However, beneficial effects of RVT against early exposure to endocrine disrupting chemicals (EDCs) have not been understood. EDCs are linked to several ovarian diseases such as premature ovarian failure, polycystic ovary syndrome, early menopause and infertility in women. Hexavalent chromium (CrVI) is a heavy metal EDC, and widely used in >50 industries. Environmental contamination with CrVI in the US is rapidly increasing, predisposing the human to several illnesses including cancers and still birth. Our lab has been involved in determining the molecular mechanism of CrVI-induced female infertility and intervention strategies to mitigate CrVI effects. Lactating mother rats were exposed to CrVI (50 ppm potassium dichromate) from postpartum days 1–21 through drinking water with or without RVT (10 mg/kg body wt., through oral gavage daily). During this time, F1 females received respective treatments through mother's milk. On postnatal day (PND) 25, blood and the ovary, kidney and liver were collected from the F1 females for analyses. CrVI increased atresia of follicles by increasing cytochrome C and cleaved caspase-3; decreasing antiapoptotic proteins; decreasing estradiol (E₂) biosynthesis and enhancing metabolic clearance of E₂, increasing oxidative stress and decreasing endogenous antioxidants. RVT mitigated the effects of CrVI by upregulating cell survival proteins and AOXs; and restored E₂ levels by inhibiting hydroxylation, glucuronidation and sulphation of E₂. This is the first study to report the protective effects of RVT against any toxicant in the ovary.

Keywords

Ovary; Chromium; Resveratrol; Antioxidants; Oxidative Stress; Steroidogenesis

^{*}Corresponding author at: Department of Veterinary Integrative Biosciences, College of Veterinary Medicine and Biomedical Sciences, TAMU 4458, Texas A&M University, College Station, TX 77843, USA. skbanu@cvm.tamu.edu (S.K. Banu).

Disclosure statement

The authors have nothing to disclose.

Transparency Document

The Transparency document associated with this article can found, in online version.

1. Introduction

Resveratrol (RVT) (3,4', 5-trihydroxystilbene), a polyphenolic component in grapes, has been known for its cytoprotective actions against neurodegeneration, cardiovascular disease, cancer, diabetes, and obesity-related disorders (Baur and Sinclair, 2006), and for extending the lifespan of organisms (Howitz et al., 2003). It also plays several roles in anti-aging (Agarwal and Baur, 2011) and anti-inflammatory pathways (Yu et al., 2012), and ameliorating metabolic syndrome (Beaudeau et al., 2010). The diversified biological effects of RVT might be explained in part by RVT's antioxidant (AOX) properties, including increases in catalase and superoxide dismutase (SOD) activities (Rubiolo et al., 2008). The AOX effect of RVT has been shown to be due to the presence of the phenolic hydroxyl groups in its chemical structure (Leonard et al., 2003). RVT effectively scavenges hydroxyls and superoxides and protects against lipid peroxidation in cell membranes and DNA damage caused by reactive oxygen species (ROS) (Leonard et al., 2003). RVT acts through specific cell signaling pathways that lead to activation of the defensive and cytoprotective systems (Shin et al., 2009).

RVT is known to have differential (and even opposite) effects based on varying physiological, pathological and pharmacological conditions in various biological systems. In cancer cells, RVT induced apoptotic cell death, and therefore is used as a chemotherapeutic agent (Garvin et al., 2006). In contrast, RVT also inhibited apoptotic cell death in certain tumor cells and other non-cancerous cell types (Manna et al., 2000; Ahmed et al., 2003). RVT attenuated apoptosis of cardiomyocytes in the heart, following ischaemia/reperfusion (Imamura et al., 2002). In rat theca interstitial cells, RVT inhibits conversion of progesterone into androgens by inhibiting steroidogenic enzymes, mainly *cyp17a1* (Ortega et al., 2012a). On the other hand, RVT increased progesterone secretion as well as mRNA levels of *Sirt1*, *LH receptor*, steroidogenic acute regulatory protein *StAR* and *Cyp19* in cultured rat granulosa cells (Morita et al., 2012b). Thus, based on the available literature, the effects of RVT seem to be specific to the cell type and physiological conditions.

Chromium (Cr) compounds are used in many industries such as leather tanning, metal plating, and other metallurgical procedures (Banu, 2013). The increased usage and inadequate disposal of Cr wastes have contributed to their increased environmental levels above safety limits. The safety level of Cr in the drinking water according to standards of the US Environmental Protection Agency (EPA) is 0.1 ppm (100 ppb) (USEPA, 2009). Whereas the drinking water or the ground water levels of Cr in some of the worst pollution incidents in the US and developing countries have been over 50–500 times the EPA limit (*e.g.*, Midland, TX, the US (5.28 ppm) (Malott, 2015), Hinkley, CA (5.0 ppm) (ContaminatedRealty, 2015), Leon, Mexico (50 ppm) (Armienta-Hernández and Rodríguez-Castillo, 1995), China (Zhang and Li, 1987) and India (31–50 ppm) (Dubey et al., 2001; Rao et al., 2011). Occupational exposure to Cr is found among approximately half a million industrial workers in the US and several millions worldwide. Significant contamination with CrVI has been found in approximately 30% of the drinking water sources in California (McNeill et al., 2012). The deposition of CrVI wastes in landfills and waterways by chromate industries affects millions of people drinking Cr-containing water and residing in the vicinity of dangerously polluted sites (Blacksmith-Institute, 2015). Cr can leach as deep

as 160 ft in the soil and can contaminate the ground water (Gordon, 2003; Webster, 2012). Women working in Cr industries and living around Cr contaminated areas experience abnormal menses, postnatal hemorrhage and birth complications with high levels of Cr in blood and urine (Shmitova, 1980), and premature abortions (Hemminki et al., 1980; Hemminki et al., 1983).

CrVI rapidly crosses the cell membranes through anionic sulphate-ion transporters. Once inside the cells, CrVI is readily converted into CrIII by AOXs such as ascorbate, glutathione (GSH), and cysteine. CrIII was initially thought to be relatively non-toxic, however, it was found to be more damaging than CrVI in causing genotoxicity in cell free systems (Fang et al., 2014). CrIII interacts with DNA and induces DNA strand breaks, DNA-protein crosslinks and oxidative DNA base modifications (Nickens et al., 2010; Fang et al., 2014). Oxidation of DNA can result in damage to all four bases of deoxyribose.

Our previous findings reported oxidative stress, activation of p53 and mitochondria-mediated intrinsic apoptosis as major pathways of CrVI to cause follicle atresia (Banu et al., 2011; Stanley et al., 2013). CrVI also caused POF in F1 offspring by disrupting POF marker protein X-prolyl aminopeptidase-2 in a rat model (Banu et al., 2015). A recent study by Lim et al. reports that increased ovarian oxidative stress in young *Gclm* knock-out mice suffer from ovarian failure due to an accelerated decline in ovarian follicles mediated by increased recruitment of follicles into the growing pool, followed by apoptosis at later stages of follicular development (Lim et al., 2015). We have recently shown that AOXs, vitamin C and edaravone mitigated CrVI-induced ovarian toxicity (Banu et al., 2008; Stanley et al., 2011; Stanley et al., 2013; Stanley et al., 2014). In the current study, we determined the protective effects of RVT on CrVI-induced ovarian toxicity, and estradiol turnover. The objectives of the study were to evaluate the protective effects of RVT on cell death and survival pathways, atresia of primordial, primary, secondary and antral follicles, ROS production and AOX enzymes. We also evaluated for the first time the effects of CrVI on the metabolic clearance of E₂ and mitigative effects of RVT.

2. Materials and methods

2.1. Materials

The reagents used in this study were purchased from the following suppliers: potassium dichromate (K₂Cr₂O₇, Cat. No. P2588) and resveratrol (3,4',5-trihydroxy-*trans*-stilbene, Cat. No. R5010) (Sigma-Aldrich, St. Louis, MO). The other chemicals used were molecular biologic grade purchased from Fisher Scientific (Pittsburgh, PA) or Sigma-Aldrich (St. Louis, MO). Details of sources of antibodies, catalog numbers, dilutions, host species, immunogens, and homologies with rat/mouse are given in Table 1.

2.2. Animals

Timed pregnant Sprague-Dawley rats were purchased from Charles River Laboratories and maintained in AAALAC-approved animal facilities with a 12 h light/12 h dark regime at 23–25 °C, and provided with Teklad 6% mouse/rat diet and water *ad libitum*. Animal Use Protocols were performed in accordance with the NIH Guidelines for the Care and Use of

Laboratory Animals, and were in accordance with the standards established by Guiding Principles in the Use of Animals in Toxicology and specific guidelines and standards of the Society for the Study of Reproduction, and approved by the Animal Care and Use Committee (IACUC) of Texas A&M University.

2.3. In vivo dosing and experimental design

The *in vivo* CrVI dosing used in this investigation was chosen based on Cr levels in drinking water in highly polluted regions in developing countries that range from 19 to 50 ppm (Zhang and Li, 1987; Armienta-Hernández and Rodríguez-Castillo, 1995; Dubey et al., 2001; Dominik et al., 2007; Rao et al., 2011). The RVT dose was chosen based on doses and dose-response studies reported in literature using rodent models (Juan et al., 2005; Macarulla et al., 2009; Johnson et al., 2011; Asadi et al., 2015). Lactating rats were divided into the following groups: (1) Control (n = 10): rats received regular drinking water; (2) CrVI treatment (n = 10): rats received potassium dichromate (CrVI, 50 ppm) dissolved in drinking water. (3) CrVI + Resveratrol (RVT) treatment (n = 10): rats received 50 ppm CrVI with RVT (10 mg/kg body wt., through oral gavage daily). On the day of birth, male pups were removed and the litters were culled to 4 female pups per mother rat, thus each treatment group consisted of 10 mothers (F0) and 10 litters for each group. In cases where fewer than 4 female pups were delivered, additional pups were fostered from other litters. In all experimental groups, the lactating mother rats received CrVI treatment in drinking water from the day of parturition to day 21 postpartum. During this period, the F1 offspring received respective treatments through the mother's milk. On postnatal day (PND) 25, female pups from each group were euthanized under CO₂ anesthesia followed by cervical dislocation, and blood and ovaries, kidney and liver were collected for further analyses. Ovaries from 10 litters (F1 pups) per group were separately assigned and analyzed as follow: (i) twenty ovaries from 5 litters (4 ovaries from each litter) were fixed in 4% paraformaldehyde for TUNEL apoptotic assay and IHC; (ii) forty ovaries from 5 litters (8 ovaries were pooled for each sample) were homogenized and used for the assay of LPO and H₂O₂; and (iii) twenty ovaries from 5 litters (8 ovaries were pooled for each sample) were used for RNA isolation and RT-PCR.

2.4. Histology and evaluation of follicular atresia

Ovaries were collected and fixed in 4% buffered paraformaldehyde for 24 h and transferred to 70% ethanol. Histological processing of the ovary was performed by the Histology core lab facility, College of Veterinary Medicine & Biomedical Sciences, Texas A&M University, based on the standard protocols for paraffin-embedded sections that were cut at 5 µm thickness and stained with hematoxylin and eosin (H&E). Every 12th section was used to count atretic follicle numbers (Devine et al., 2002). Atresia of primordial, primary, secondary and antral follicles was counted separately from both the ovaries and expressed in percentage of total follicles. The criteria to identify atretic follicles were according to Osman (Osman, 1985) and Borgeest et al., (Borgeest et al., 2002) as follows: degenerative changes in the GC wall which shows cell shrinkage, pyknosis, and karyorrhexis (rupture of nucleus with disintegration of chromatin into granules); and/or degenerative changes in the oocyte such as the breakdown of the nuclear membrane with oocyte fragmentation. Antral follicles

were considered atretic if they contained disorganized GC with at least 20 apoptotic bodies in the GC layer(s).

2.5. Terminal deoxynucleotidyl transferase dUTP nick end labeling (TUNEL) assay

Paraffin-embedded tissue sections were deparaffinized and TUNEL assay was performed as previously described (Sivakumar et al., 2014; Stanley et al., 2015). The apoptotic index (AI) was calculated as the average percentage of TUNEL-positive oocytes and granulosa cells from the ovaries at 400× magnification.

2.6. Immunohistochemistry

Paraffin-embedded tissue sections were deparaffinized and IHC was performed as previously described (Stanley et al., 2014; Banu et al., 2015). The intensity of staining for each protein was quantified using Image-ProPlus 6.3 image processing and analysis software according to the manufacturer's instructions (Media Cybernetics, Inc.; Bethesda, MD). In brief: six images of the ovary at 400× magnification were captured randomly without bias in each tissue section per animal. Integrated Optical Density (IOD) of immunostaining was quantified in the RGB mode. Numerical data were expressed as least square mean ± SEM. This technique is more quantitative than conventional blind scoring systems and the validity of the quantification was reported previously by our group (Lee et al., 2012).

2.7. Measurement of steroid hormones

Serum levels of progesterone (P4), testosterone (T) and estradiol (E₂) were estimated in F1 female pups on PND 25 using ELISA kits (DRG Diagnostics) according to the manufacturer's instructions. The sensitivities of the assays for P4, T and E₂ were 0.04 ng/ml, 0.06 ng/ml and 9.0 pg/ml respectively. The intra-assay and inter-assay coefficients of variation ranged from 4.0% to 7.3%.

2.8. Measurement of oxidative damage in the ovary

Oxidative damage was measured by estimating the levels of hydrogen peroxide (H₂O₂) and lipid peroxide (LPO) in the ovary and serum as described (Stanley et al., 2013). Briefly, ovaries were dissected out and homogenized in 50 mM Tris-HCl buffer, pH 7.5, and centrifuged at 10,000 ×g for 15 min. The supernatants were used for the assay. LPO and H₂O₂ production was measured spectrophotometrically using a commercial kit (Cayman Chemical).

2.9. Real-time reverse transcription (RT)-polymerase chain reaction (PCR)

Total RNA was isolated from the ovary, kidney and the liver using RNeasy Mini Kit (Cat. No. 74104, Qiagen, USA) according to manufacturer's instructions. The purity and concentration of RNA was determined spectrophotometrically by measuring the absorbance at 260/280 nm and a purity of 1.8–2.0 was considered acceptable for the real time RT-PCR analysis. The first strand cDNA was synthesized using 100 ng total RNA by QuantiTect RT kit (Cat. 205311, Qiagen, USA) according to manufacturer's instructions. Real-time PCR was performed using the Power SYBR®Green master mix (Cat. 4368577, Life Technologies, USA) according to manufacturer's instructions. cDNA (2 µl) was mixed with

10 µl master mix (dNTP mix, AmpliTaq Gold® DNA polymerase, optimized buffer components and SYBR®Green I dye), sense and anti-sense oligonucleotide primers for respective genes and β-actin gene for internal control, with the total reaction volume made up to 20 µl with RNase free water. The reaction cycles were as follows: PCR enzyme initial activation at 95 °C for 15 min; initial denaturation at 94 °C for 15 s, annealing at 60 °C for 30 s and elongation at 72 °C for 30 s. All reactions were run in triplicate. The PCR amplification of all transcripts was performed on the Step-One Plus real-time PCR machine (Life Technologies, Carlsbad, CA). The fold differences were calculated by normalizing the relative expression of gene of interest with β-actin and the results were expressed as fold changes. Details of the sense and anti-sense oligonucleotide primer sequences used for the real-time PCR analysis were given in Table 2. Relative gene expression was presented by comparative CT (also referred to as the $\Delta\Delta CT$) method (Schmittgen and Livak, 2008).

2.10. Statistical analyses

All the numerical data were subjected to one-way ANOVA to detect the effects of treatment and dose interactions. The Tukey-Kramer HSD test was used to adjust for multiple pair-wise comparisons of means. We take into account the nested structure in the design. Mixed models analysis was used to account for any correlation between the results of pups from the same dam. Mixed models were used to model both fixed effects (in this case treatment) and random effects (in this case dams and pups) (Kratzer and Littell, 2006; Littell et al., 2006). Statistical analyses were performed using general linear models of Statistical Analysis System (SAS, Cary, NC) and $P < 0.05$ was considered significant.

3. Results

3.1. Effects of resveratrol on CrVI-induced follicle atresia and apoptosis of oocytes and granulosa cells

Primordial, primary, secondary and antral follicle numbers were counted in serial sections of the ovary. Control ovaries had several healthy follicles (Fig. 1A, D and G). Lactational exposure to CrVI significantly increased atresia of primordial, primary, secondary and antral follicles (Fig. 1B, E and H; J–M). Supplementation with RVT mitigated CrVI-induced increase in follicle atresia (Fig. 1C, F, I; J–M). Results from the TUNEL in situ apoptotic assay revealed that CrVI significantly increased apoptosis of oocytes and granulosa cells in the primordial, primary, secondary and antral follicles (Fig. 2B, E and H; J–M). RVT significantly rescued both the oocytes and granulosa cells from CrVI-induced increase in apoptosis (Fig. 2C, F and I; J–M).

3.2. Effects of resveratrol on CrVI-induced cell death and cell survival pathways

In order to understand the mechanism behind CrVI-induced increase in follicle atresia, we determined proteins involved in cell death and cell survival. CrVI significantly ($P < 0.01$) upregulated cytochrome C and cleaved caspase-3 compared to control, and RVT mitigated the adverse effects of CrVI (Fig. 3A–H). Cell survival proteins Bcl-2, Bcl-XL and Hypoxia-inducible factor 1-alpha (HIF1α) were significantly decreased by CrVI. However, RVT effectively inhibited the CrVI effects on Bcl-2 and HIF1α, but not on Bcl-XL (Fig. 3I–T).

3.3. Effects of resveratrol on CrVI-induced oxidative stress and antioxidant enzymes

Lactational exposure to CrVI significantly increased the activities of oxidative stress markers LPO and H₂O₂ in the plasma and the ovary. However, RVT mitigated the effects of CrVI on LPO and H₂O₂ activities (Fig. 4A–D).

Further, we determined the effects of RVT on the expression of cytosolic AOX enzymes glutathione peroxidase (GPx) 1, superoxide dismutase (SOD) 1 and catalase. GPx1 was highly expressed in oocytes and granulosa cells of the antral follicles in control ovaries. CrVI significantly decreased the expression of GPx1. Supplementation with RVT inhibited the effects of CrVI on the ovary, and enhanced GPx1 in the oocytes more than the control group (Figs. 5A–D). Catalase was highly expressed in granulosa cells and oocytes in control ovaries. CrVI downregulated catalase. Supplementation with RVT highly upregulated catalase expression in granulosa cells, and the expression levels were higher than both the control and CrVI groups (Fig. 5E–H). In contrast, CrVI upregulated SOD1 compared to control; and RVT supplementation to CrVI-treated rats further increased SOD1 expression in the ovary compared to control and CrVI groups (Fig. 5I–L). We also measured the expression of mitochondrial AOX enzymes SOD2, peroxiredoxin (PRDX) 3 and thioredoxin (TXN) 2. SOD2 showed a similar response to CrVI and CrVI + RVT as that of SOD1 (Fig. 5M–P). Control ovaries highly expressed PRDX3 and TXN2, and CrVI downregulated both the enzymes. Supplementation with RVT mitigated the adverse effects of CrVI on PRDX3 and TXN2 (Fig. 5Q–X).

3.4. Effects of resveratrol on CrVI-induced changes in the biosynthesis of E₂

Lactational exposure to CrVI significantly decreased P4, T and E₂ levels in the serum. RVT significantly mitigated the effects of CrVI (Fig. 6). In order to understand the mechanism by which levels of steroids were reduced, we measured the abundance of StAR, 3βHSD and aromatase (Cyp19) proteins in the ovary. CrVI downregulated StAR, 3βHSD and p450 aromatase proteins. RVT mitigated the effects of CrVI on the expression of StAR and aromatase, but not on 3βHSD (Fig. 7A–L).

3.5. Effects of resveratrol on CrVI-induced metabolic clearance of E₂

Finally, we determined effects of RVT on catabolic pathways of E₂. Estrogen is catabolized through three major pathways, UDP-glucuronidation, sulfation and hydroxylation, mainly in the liver and kidney. Conversion of E₂ into 2-hydroxyestradiol (OHE₂) and/or 4-OHE₂ is catalyzed by Cyp1a1 and Cyp1b1. CrVI significantly increased *Cyp1a1* and *Cyp1b1*, which was mitigated by RVT (Fig. 8A, B and C) in the ovary, kidney and liver. UDP-glucuronosyltransferases (UGTs), important phase II drug-metabolizing enzymes, convert E₂ into 2/4-OHE₂ glucuronides (Raftogianis et al., 2000) (Fig. 9). CrVI upregulated *Ugt1a1*, *Ugt1a3*, and *Ugt1a9*, which was mitigated by RVT. *Sult1a1* converts E₂ or OHE₂ into E₂ sulphate or OHE₂-OH-sulphate (Dawson, 2012). CrVI upregulated *Sult1a1* in the ovary, kidney and the liver, and RVT mitigated the effects of CrVI (Figs. 8A, B and C; 9). NAD(P)H quinone oxidoreductase 1 (Nqo1) is implicated in the oxidation of estrogens to quinones that react with DNA (Gaikwad et al., 2007). CrVI upregulated *Nqo1* and RVT mitigated the effect of Nqo1. Glutathione (GSH)-S-transferases (*Gstm1*, *Gstm2*, and *Gsta4*) play key roles in the cellular detoxification of electrophilic compounds through GSH

conjugation and in protection against lipid peroxidation (Townsend et al., 2003). CrVI downregulated these enzymes, and RVT effectively mitigated the effects of CrVI (Fig. 8A, B and C). Fig. 9 summarizes the key E₂ metabolic pathways that are enhanced by CrVI and mitigated by RVT, resulting in the partial restoration of E₂ levels against CrVI toxicity.

4. Discussion

Our previous studies have shown that vitamin C (ascorbate) and ROS scavenger edaravone mitigated CrVI-induced toxicity in the ovaries (Banu et al., 2008; Stanley et al., 2013; Stanley et al., 2014). Few studies are available on the effects of RVT on heavy-metal toxicity. Notably, RVT protected mice from arsenic trioxide-induced cardiotoxicity both *in vivo* and *in vitro* (Zhao et al., 2008). In RAW 264.7 (mouse leukemic monocyte macrophage) cell line, RVT efficiently scavenged ·OH and O₂⁻ radicals; inhibited lipid peroxidation induced by CrIII/H₂O₂; inhibited DNA damage due to ·OH radicals produced by the Fenton reaction; and inhibited CrVI-induced NF-κB activation (Leonard et al., 2003). RVT reduced oxidative damage to purified DNA by scavenging the ·OH generated by CrIII/H₂O₂ (Burkhardt et al., 2001; Lopez-Burillo et al., 2003). While it is impossible to completely eliminate Cr from the environment, there is a pressing need to identify and validate various intervention strategies to mitigate or inhibit CrVI-induced toxicity. Data from the current study demonstrate that lactational exposure to CrVI: (i) increased follicle atresia and apoptosis of oocytes and granulosa cells by increasing cell death machinery and inhibiting cell survival proteins; (ii) decreased steroid hormone biosynthesis and enhanced catabolism of E₂, thus decreasing the circulating levels of E₂; (iii) increased oxidative stress, and decreased cytoplasmic and mitochondrial AOX enzymes. Further, RVT reversed the adverse effects of CrVI on each of the above endpoints. To the best of our knowledge, this is the first study to demonstrate a protective effect of RVT on the ovary against any toxicant.

Lactational exposure to CrVI through mother's milk increased atresia of primordial and antral follicles by increasing oocyte/granulosa cell apoptosis. Interestingly, RVT protected the ovary against CrVI-induced follicle atresia. In order to understand the mechanism, we examined cell death and cell survival machinery in the ovary. Our data demonstrated that CrVI increased follicle atresia by increasing the levels of cytochrome C and cleaved caspase 3, implicating the mitochondria-mediated intrinsic apoptosis. Further, results also showed a marked decrease in cell survival/anti-apoptotic machinery such as Bcl-2, Bcl-XL and HIF1α due to CrVI treatment. Whereas, RVT restored Bcl-2 and HIF1α. In support of these data, a similar study showed that pretreatment of irradiated rats with RVT at different doses significantly protected the ovarian follicle counts and markedly increased the AOX enzymes (Simsek et al., 2012). RVT effectively protected the ovarian follicular reserve by inhibiting follicular atresia in aging rats (Chen et al., 2010). In contrast RVT displayed an apoptotic effect on theca interstitial cells. RVT also reduced androgen production of theca interna cells by decreasing *Cyp 17a1* and Akt/PKB phosphorylation (Ortega et al., 2012a; Ortega et al., 2014). RVT showed a cardioprotective effect, displaying AOX, anti-apoptotic and antiarrhythmic effects in mice (Das and Maulik, 2006; Zhang et al., 2006). Taken together, RVT seems to display a concentration- and cell type-dependent induction of both pro- and anti-apoptotic mechanisms (Clement et al., 1998; Lee et al., 2006; Ungvari et al., 2007).

A recent report showed that RVT attenuated iron-induced oxidative stress in the sperm of CD1⁺ mice through the inhibition of mitochondrial impairment and ROS production (Mojica-Villegas et al., 2014). RVT, being a natural polyphenolic compound and a potent AOX, has the capacity to inhibit both mitochondrial ROS production and permeability transition (Lin et al., 2014; Gibellini et al., 2015). RVT was able to scavenge ·OH radicals produced by JB6 cells exposed to CrVI (Leonard et al., 2003). Lipid peroxidation in cell membranes caused by ·OH radicals and DNA damage due to ·OH radicals produced by the Fenton reaction were inhibited by RVT (Leonard et al., 2003). In support of the above reports, the current study showed that RVT protected the ovary against CrVI-induced increase in oxidative stress by decreasing LPO and H₂O₂ in the plasma and the ovary.

Cytoprotective effects of RVT results from scavenging of ROS as well as activation of several specific signaling pathways that enable cells to promote AOX defense system. We therefore determined the expression of cytoplasmic and mitochondrial AOX enzymes at the protein level. RVT highly restored CrVI-induced decrease in cytoplasmic AOXs such as GPx1 and catalase; and mitochondrial AOXs PRDX3 and TXN2. Interestingly, CrVI upregulated SOD1 and SOD2 while decreasing other AOXs compared to control ovaries. RVT did not reverse the effects of CrVI; rather, it enhanced SOD1 and 2 compared to control and CrVI. RVT increased GSH synthesis (Kode et al., 2008) and activated catalase, SOD, and NQO1 (Rubiolo et al., 2008) in rat hepatocytes. Overall, we speculate that RVT may have protected the follicles from CrVI-induced oxidative stress by increasing the transcription, translation and/or activity of endogenous AOX enzymes.

We also evaluated the protective effects of RVT against CrVI-induced decrease in ovarian steroidogenesis. Our data indicate that lactational exposure to CrVI through mother's milk decreased P₄, T and E₂ whereas supplementation of RVT to CrVI-exposed rats restored P₄, T and E₂ levels. Previous reports indicated several discrepancies on the effects of RVT on steroid biosynthetic pathways (Supornsilchai et al., 2005; Svechnikov et al., 2009; Morita et al., 2012b; Ortega et al., 2012b; Li et al., 2014; Ortega and Duleba, 2015). A majority of the literature identifies inhibitory effects of RVT on steroidogenesis and/or aromatization of androgens in rat adrenocortical cells (Supornsilchai et al., 2005), Leydig cells (Svechnikov et al., 2009) and theca cells (Ortega et al., 2012b). In contrast, Morita et al. (Morita et al., 2012b) reported that RVT increased mRNA levels of *Sirt1*, *LH receptor*, *StAR*, and *P450 aromatase* in rat granulosa cells. In the current study CrVI significantly decreased protein levels of StAR, P450 aromatase and 3βHSD in the ovary, however, RVT restored CrVI-induced decrease in StAR and P450 aromatase in the ovary, but not 3βHSD. A recent study indicated that RVT inhibits LH-induced androgen production in immature rat Leydig cells by inhibiting 3βHSD (Li et al., 2014). However, additional data on the other steroid biosynthetic enzymes including 17βHSD as well as the role of RVT on the interaction between granulosa and theca cells in steroid biosynthesis are needed in order to confirm the specific role of RVT on steroid biosynthetic pathway. Future studies will focus on a comprehensive analysis of RVT on the integrated role(s) of granulosa and theca cells-specific steroidogenic pathways.

RVT was unable to mitigate the effects of CrVI on ERβ protein levels. RVT showed a non-specific binding with ERs in the brain (Shin et al., 2015) to protect the brains of estrogen-

deficient females against ischemic insult. A vast majority of the research involving synthetic or natural (phyto) estrogens are targeted on ER-signaling. Few studies have provided strong evidence for the existence of ER-independent pathways leading to endocrine disruption (Hanet et al., 2008). Since the mechanism of RVT in restoring E₂ levels remained unclear, we attempted to evaluate the effects of RVT on metabolic clearance of E₂. The metabolism of estrogen takes place primarily in the liver through phase I (hydroxylation) and phase II (methylation, glucuronidation, and sulfation) pathways, with final excretion in the urine and feces (Hall, 2001).

Cytochrome P450 enzymes mediate the hydroxylation of E₂ and estrone, which is the major Phase I metabolic pathway for endogenous estrogens (Martucci and Fishman, 1993). This takes place at the 2 carbon (C-2) position producing 2-hydroxyestradiol (2-OHE₂) or at the 16a carbon (C-16a) position or 4 carbon (C-4) position giving rise to 16a-OHE₂ and 4-OHE₂, respectively (Martucci and Fishman, 1993). Conversion of E₂ into 2-OHE₂ and/or 4-OHE₂ is catalyzed by Cyp1a1 and Cyp1b1. Cyp1b1 is highly expressed in estrogen-responsive tissues, such as mammary gland, uterus, and ovary (Hakkola et al., 1997), suggesting that Cyp1b1 is important in the local control of estrogen metabolism. Our data indicated that CrVI significantly increased *Cyp1a1* and *Cyp1b1* mRNA expressions in the ovary, liver and kidney. However, supplementation of RVT effectively inhibited the effects of CrVI on these enzymes. A study in cultured human mammary epithelial cells showed that RVT inhibited TCDD-induced expression of Cyp1a1 and Cyp1b1 and catechol estrogen-mediated oxidative DNA damage (Chen et al., 2004). Thus our study suggests that RVT may provide a potential intervention against CrVI toxicity through the suppression of *Cyp1a1* and *Cyp1b1*.

We further determined the effects of RVT on phase II metabolic pathways such as glucuronidation and sulfation. UGTs are important phase II drug-metabolizing enzymes involved in the metabolism of endogenous compounds including E₂ (Raftogianis et al., 2000). CrVI significantly increased *Ugt1a1*, *Ugt1a2*, *Ugt1a3* and *Ugt1a9* (but not *Ugt2b7*, data not shown). Interestingly, RVT inhibited the effects of CrVI on UGTs in the ovary, kidney and liver. Sult1a1 is responsible for estrogen and catecholesterogen sulphation (Huber et al., 2010). Sult1a1 also catalyzes the sulfation of 2-methoxyestradiol, an endogenous, potent antiestrogen (Spink et al., 2000). Our data indicate that CrVI upregulated *Sult1a1* mRNA, and RVT significantly inhibited the effects of CrVI on *Sult1a1* in the ovary, kidney and liver.

CrVI is known to increase ROS (Banu, 2013). Cyp1b1 and NAD(P)H quinone oxidoreductase 1 (Nqo1) are implicated in the oxidation of estrogens to quinones that react with DNA to form predominantly depurinating DNA adducts (Shimada et al., 1996; Talalay et al., 2003). Nqo1 promotes p53 accumulation in an MDM2 and ubiquitin independent manner, which reinforces the cellular senescence phenotype (Liu et al., 2015). Interestingly, CrVI increased *Nqo1* expression in the ovary, liver and kidney. RVT mitigated the effects of CrVI in the ovary, inhibited CrVI effects in the kidney and the liver. Our previous findings documented that CrVI increased the expression, phosphorylation, mitochondrial translocation, and stabilization of p53 in the ovary (Banu et al., 2011; Sivakumar et al., 2014; Stanley et al., 2015). CrVI-induced increase in *Nqo1* expression could be one of the

possible mechanisms for the activation and stabilization of p53. GSTs catalyzes GSH conjugation of E₂-semiquinones, enhances cellular detoxification of electrophilic compounds and protects against lipid peroxidation (Raftogianis et al., 2000). CrVI down regulated *Gstm1*, *Gstm2*, and *Gsta4* which is restored by RVT.

Interestingly, RVT completely rescued the ovary from the CrVI-induced increase in ROS, apoptosis, and steroid metabolic enzymes; as well as the decrease in AOXs and inhibition of cell survival machinery. However, RVT partially rescued the ovary from the CrVI-induced follicle atresia and steroidogenesis, rendering intervention selective to specific endpoints. RVT is well absorbed, however, it undergoes an extensive sulfation and glucuronidation in the duodenum and liver, rendering an average half-life of 1.5 h (Yu et al., 2002; Rocha-Gonzalez et al., 2008). Thus, dosing the dams or pups every 12 h instead of 24 h may increase its potential against follicle atresia and/or steroidogenesis. RVT directly modulates mRNA levels of several genes such as *Sirt1*, *LH receptor*, *StAR*, and *P450 aromatase* in rat granulosa cells (Morita et al., 2012a). Therefore, one of the reasons for the preferential intervention may be the differential gene expression pattern, namely, the steroidogenesis panel, steroid metabolic panel, cell survival and/or apoptotic panel in response to RVT.

As illustrated in Fig. 9, the collective data on E₂ metabolism in the current study show that: (i) CrVI potentially increased E₂ hydroxylation, glucuronidation and sulphation as well as formation of E₂-semiquinones by upregulating phase I/II metabolic cytochrome P450 enzymes; (ii) RVT, as a potent AOX and a phytoestrogen, rendered a protective effect against the CrVI in restoring E₂ levels by means of inhibiting phase I/II metabolic cytochrome P450 enzymes in the ovary, kidney and the liver. (iii) In contrast, RVT was not able to increase 3βHSD. Thus, apart from its AOX effects, RVT seems to have a direct effect on regulating gene transcription of E₂ metabolic pathways. Ongoing and the future studies in our lab will explore more on the effects of RVT against CrVI toxicity in terms of steroidogenesis and granulosa cell interaction in steroidogenesis. Therefore, this is the first study to address the protective effect of RVT against Cr toxicity in any biological system.

Acknowledgments

This work was supported by National Institute of Environmental Health Sciences (NIEHS) grants ES020561-01 and ES025234-01A1 (S.K.B.) and the Center for Translational Environmental Health Research (CTEHR, P30ES023512) (S.K.B., R.C.B). Microscopy was performed in the Texas A&M University College of Veterinary Medicine & Biomedical Sciences Image Analysis Laboratory, supported by an NIH-NCRR Shared Instrumentation Grant (R.C.B.) (1 S10 RR22532-01). Authors gratefully acknowledge Thamizh K. Nithy for her assistance with figures.

References

- Agarwal B, Baur JA. Resveratrol and life extension. *Ann N Y Acad Sci.* 2011; 1215:138–143. [PubMed: 21261652]
- Ahmed KA, Clement MV, Pervaiz S. Pro-oxidant activity of low doses of resveratrol inhibits hydrogen peroxide—induced apoptosis. *Ann N Y Acad Sci.* 2003; 1010:365–373. [PubMed: 15033754]
- Armienta-Hernández MA, Rodríguez-Castillo R. Environmental exposure to chromium compounds in the valley of León, México. *Environ Health Perspect.* 1995; 103:47–51.

- Asadi S, Goodarzi MT, Saidijam M, Karimi J, Azari RY, Farimani AR, Salehi I. Resveratrol attenuates visfatin and vaspin genes expression in adipose tissue of rats with type 2 diabetes. *Iran Bosn J Basic Med Sci.* 2015; 18:537.
- Banu, SK. Heavy metals and the ovary. In: Hoyer, PB., editor. *Ovarian Toxicology*. 2. CRC Press; 2013. p. 191-228.
- Banu SK, Samuel JB, Arosh JA, Burghardt RC, Aruldas MM. Lactational exposure to hexavalent chromium delays puberty by impairing ovarian development, steroidogenesis and pituitary hormone synthesis in developing Wistar rats. *Toxicol Appl Pharmacol.* 2008; 232:180–189. [PubMed: 18602937]
- Banu SK, Stanley JA, Lee J, Stephen SD, Arosh JA, Hoyer PB, Burghardt RC. Hexavalent chromium-induced apoptosis of granulosa cells involves selective sub-cellular translocation of Bcl-2 members, ERK1/2 and p53. *Toxicol Appl Pharmacol.* 2011; 251:253–266. [PubMed: 21262251]
- Banu SK, Stanley JA, Sivakumar KK, Arosh JA, Barhouni R, Burghardt RC. Identifying a novel role for X-prolyl aminopeptidase (Xpnpep) 2 in CrVI-induced adverse effects on germ cell nest breakdown and follicle development in rats. *Biol Reprod.* 2015; 92:67. [PubMed: 25568306]
- Baur JA, Sinclair DA. Therapeutic potential of resveratrol: the in vivo evidence. *Nat Rev Drug Discov.* 2006; 5:493–506. [PubMed: 16732220]
- Beaudeau JL, Nivet-antoine V, Giral P. Resveratrol: a relevant pharmacological approach for the treatment of metabolic syndrome? *Curr Opin Clin Nutr Metab Care.* 2010; 13:729–736. [PubMed: 20823772]
- Blacksmith-Institute. Pure Earth and Green Cross Switzerland. The Blacksmith Institute; New York City, USA: 2015. *World Worst Pollution Problems*; p. 1-36.
- Borgeest C, Symonds D, Mayer LP, Hoyer PB, Flaws JA. Methoxychlor may cause ovarian follicular atresia and proliferation of the ovarian epithelium in the mouse. *Toxicol Sci.* 2002; 68:473–478. [PubMed: 12151644]
- Burkhardt S, Reiter RJ, Tan DX, Hardeland R, Cabrera J, Karbownik M. DNA oxidatively damaged by chromium(III) and H₂O₂ is protected by the antioxidants melatonin, N(1)-acetyl-N(2)-formyl-5-methoxykynuramine, resveratrol and uric acid. *Int J Biochem Cell Biol.* 2001; 33:775–783. [PubMed: 11404181]
- Chen ZH, Hurh YJ, Na HK, Kim JH, Chun YJ, Kim DH, Kang KS, Cho MH, Surh YJ. Resveratrol inhibits TCDD-induced expression of CYP1A1 and CYP1B1 and catechol estrogen-mediated oxidative DNA damage in cultured human mammary epithelial cells. *Carcinogenesis.* 2004; 25:2005–2013. [PubMed: 15142886]
- Chen ZG, Luo LL, Xu JJ, Zhuang XL, Kong XX, Fu YC. Effects of plant polyphenols on ovarian follicular reserve in aging rats. This paper is one of a selection of papers published in this special issue entitled “Second International Symposium on Recent Advances in Basic, Clinical, and Social Medicine” and has undergone the Journal’s usual peer review process. *Biochem Cell Biol.* 2010; 88:737–745. [PubMed: 20651847]
- Clement MV, Hirpara JL, Chawdhury SH, Pervaiz S. Chemopreventive agent resveratrol, a natural product derived from grapes, triggers CD95 signaling-dependent apoptosis in human tumor cells. *Blood.* 1998; 92:996–1002. [PubMed: 9680369]
- ContaminatedRealty. victims town of hinkley. Hinkley, CA: 2015. <http://www.victimstowntofhinkley.org/>
- Das DK, Maulik N. Resveratrol in cardioprotection: a therapeutic promise of alternative medicine. *Mol Interv.* 2006; 6:36–47. [PubMed: 16507749]
- Dawson, AP. The biological roles of steroid sulfonation. In: Sergej, MO., editor. *Steroids — From Physiology to Clinical Medicine*. 2012. p. 45-64.
- Devine PJ, Sipes IG, Skinner MK, Hoyer PB. Characterization of a rat in vitro ovarian culture system to study the ovarian toxicant 4-vinylcyclohexene diepoxide. *Toxicol Appl Pharmacol.* 2002; 184:107–115. [PubMed: 12408955]
- Dominik J, Vignati DAL, Koukal B, Pereira de Abreu MH, Kottelat R, Szalinska E, Ba B, Bobrowski A. Speciation and environmental fate of chromium in rivers contaminated with tannery effluents. *Eng Life Sci.* 2007; 7:155–169.

- Dubey C, Sahoo B, Nayak N. Chromium (VI) in waters in parts of Sukinda chromite valley and health hazards, Orissa, India. *Bull Environ Contam Toxicol*. 2001; 67:541–548. [PubMed: 11779069]
- Fang Z, Zhao M, Zhen H, Chen L, Shi P, Huang Z. Genotoxicity of tri- and hexavalent chromium compounds in vivo and their modes of action on DNA damage in vitro. *PLoS One*. 2014; 9:e103194. [PubMed: 25111056]
- Gaikwad NW, Rogan EG, Cavalieri EL. Evidence from ESI-MS for NQO1-catalyzed reduction of estrogen orthoquinones. *Free Radic Biol Med*. 2007; 43:1289–1298. [PubMed: 17893042]
- Garvin S, Öllinger K, Dabrosin C. Resveratrol induces apoptosis and inhibits angiogenesis in human breast cancer xenografts in vivo. *Cancer Lett*. 2006; 231:113–122. [PubMed: 16356836]
- Gibellini L, Bianchini E, De Biasi S, Nasi M, Cossarizza A, Pinti M. Natural compounds modulating mitochondrial functions. *Evid Based Complement Alternat Med*. 2015; 2015:1–13.
- Gordon, TR. U. S. Environmental Protection Agency – Region 2. New York, NY: 2003. Documentation of environmental indicator determination — Interim Final 2/5/99; p. 1-19.
- Hakkola J, Pasanen M, Pelkonen O, Hukkanen J, Evisalmi S, Anttila S, Rane A, Mantyla M, Purkunen R, Saarikoski S, Tooming M, Raunio H. Expression of CYP1B1 in human adult and fetal tissues and differential inducibility of CYP1B1 and CYP1A1 by Ah receptor ligands in human placenta and cultured cells. *Carcinogenesis*. 1997; 18:391–397. [PubMed: 9054634]
- Hall D. Nutritional influences on estrogen metabolism. *Appl Nutr Sci Rep*. 2001; 1:1–8.
- Hanet N, Lancon A, Delmas D, Jannin B, Chagnon MC, Cherkaoui-Malki M, Latruffe N, Artur Y, Heydel JM. Effects of endocrine disruptors on genes associated with 17beta-estradiol metabolism and excretion. *Steroids*. 2008; 73:1242–1251. [PubMed: 18634814]
- Hemminki K, Niemi ML, Koskinen K, Vainio H. Spontaneous abortions among women employed in the metal industry in Finland. *Int Arch Occup Environ Health*. 1980; 47:53–60. [PubMed: 7429646]
- Hemminki K, Kyyronen P, Niemi ML, Koskinen K, Sallmen M, Vainio H. Spontaneous abortions in an industrialized community in Finland. *Am J Public Health*. 1983; 73:32–37. [PubMed: 6847997]
- Howitz KT, Bitterman KJ, Cohen HY, Lamming DW, Lavu S, Wood JG, Zipkin RE, Chung P, Kisilewski A, Zhang LL. Small molecule activators of sirtuins extend *Saccharomyces cerevisiae* lifespan. *Nature*. 2003; 425:191–196. [PubMed: 12939617]
- Huber, J., Tempfer-Bentz, E-K., Ott, J., Tempfer, C. Estrogen-metabolizing gene polymorphisms, genetic susceptibility, and pharmacogenomics. In: Welch, P., editor. *The Role of Genetics in Breast and Reproductive Cancers*. Springer; New York: 2010. p. 285-314.
- Imamura G, Bertelli AA, Bertelli A, Otani H, Maulik N, Das DK. Pharmacological preconditioning with resveratrol: an insight with iNOS knockout mice. *Am J Physiol Heart Circ Physiol*. 2002; 282:1996–2003.
- Johnson W, Morrissey R, Osborne A, Kapetanovic I, Crowell J, Muzzio M, McCormick D. Subchronic oral toxicity and cardiovascular safety pharmacology studies of resveratrol, a naturally occurring polyphenol with cancer preventive activity. *Food Chem Toxicol*. 2011; 49:3319–3327. [PubMed: 21939727]
- Juan ME, Gonzalez-Pons E, Munuera T, Ballester J, Rodríguez-Gil JE, Planas JM. *trans*-Resveratrol, a natural antioxidant from grapes, increases sperm output in healthy rats. *J Nutr*. 2005; 135:757–760. [PubMed: 15795430]
- Kode A, Rajendrasozhan S, Caito S, Yang SR, Megson IL, Rahman I. Resveratrol induces glutathione synthesis by activation of Nrf2 and protects against cigarette smoke-mediated oxidative stress in human lung epithelial cells. *Am J Physiol Lung Cell Mol Physiol*. 2008; 294:L478–L488. [PubMed: 18162601]
- Kratzer DD, Littell RC. Appropriate statistical methods to compare dose responses of methionine sources. *Poult Sci*. 2006; 85:947–954. [PubMed: 16673777]
- Lee SC, Chan J, Clement MV, Pervaiz S. Functional proteomics of resveratrol-induced colon cancer cell apoptosis: caspase-6-mediated cleavage of lamin A is a major signaling loop. *Proteomics*. 2006; 6:2386–2394. [PubMed: 16518869]
- Lee J, Banu SK, Nithy TK, Stanley JA, Arosh JA. Early pregnancy induced expression of prostaglandin E2 receptors EP2 and EP4 in the ovine endometrium and regulated by interferon tau

through multiple cell signaling pathways. *Mol Cell Endocrinol.* 2012; 348:211–223. [PubMed: 21907262]

- Leonard SS, Xia C, Jiang BH, Stinefelt B, Klandorf H, Harris GK, Shi X. Resveratrol scavenges reactive oxygen species and effects radical-induced cellular responses. *Biochem Biophys Res Commun.* 2003; 309:1017–1026. [PubMed: 13679076]
- Li L, Chen X, Zhu Q, Chen D, Guo J, Yao W, Dong Y, Wei J, Lian Q, Ge RS, Yuan B. Disrupting androgen production of Leydig cells by resveratrol via direct inhibition of human and rat 3beta-hydroxysteroid dehydrogenase. *Toxicol Lett.* 2014; 226:14–19. [PubMed: 24472608]
- Lim J, Nakamura BN, Mohar I, Kavanagh TJ, Luderer U. Glutamate cysteine ligase modifier subunit (Gclm) null mice have increased ovarian oxidative stress and accelerated age-related ovarian failure. *Endocrinology.* 2015; 156:3329–3343. [PubMed: 26083875]
- Lin CJ, Chen TH, Yang LY, Shih CM. Resveratrol protects astrocytes against traumatic brain injury through inhibiting apoptotic and autophagic cell death. *Cell Death Dis.* 2014; 5:e1147. [PubMed: 24675465]
- Littell, RC., Stroup, WW., Milliken, GA., Wolfinger, RD., Schabenberger, O. *Mixed Model Diagnostics, SAS for Mixed Models.* SAS institute; Cary, NC, USA: 2006. p. 413-437.
- Liu K, Jin B, Wu C, Yang J, Zhan X, Wang L, Shen X, Chen J, Chen H, Mao Z. NQO1 Stabilizes p53 in response to oncogene-induced senescence. *Int J Biol Sci.* 2015; 11:762–771. [PubMed: 26078718]
- Lopez-Burillo S, Tan DX, Mayo JC, Sainz RM, Manchester LC, Reiter RJ. Melatonin, xanthurenic acid, resveratrol, EGCG, vitamin C and algalipic acid differentially reduce oxidative DNA damage induced by Fenton reagents: a study of their individual and synergistic actions. *J Pineal Res.* 2003; 34:269–277. [PubMed: 12662349]
- Macarulla M, Alberdi G, Gómez S, Tueros I, Bald C, Rodriguez V, Martínez J, Portillo M. Effects of different doses of resveratrol on body fat and serum parameters in rats fed a hypercaloric diet. *J Physiol Biochem.* 2009; 65:369–376. [PubMed: 20358350]
- Malott, V. US-Environmental-Protection-Agency. EPA Region 6: Congressional District 11. Environmental Protection Agency; 2015. West county road 112: Midland Texas; p. 1-6.
- Manna SK, Mukhopadhyay A, Aggarwal BB. Resveratrol suppresses TNF-induced activation of nuclear transcription factors NF- κ B, activator protein-1, and apoptosis: potential role of reactive oxygen intermediates and lipid peroxidation. *J Immunol.* 2000; 164:6509–6519. [PubMed: 10843709]
- Martucci CP, Fishman J. P450 enzymes of estrogen metabolism. *Pharmacol Ther.* 1993; 57:237–257. [PubMed: 8361994]
- McNeill LS, McLean JE, Parks JL, Edwards MA. Hexavalent Chromium review, part 2: chemistry, occurrence, and treatment. *J Am Water Works Assoc.* 2012; 104:E395–E405.
- Mojica-Villegas MA, Izquierdo-Vega JA, Chamorro-Cevallos G, Sanchez-Gutierrez M. Protective effect of resveratrol on biomarkers of oxidative stress induced by iron/ascorbate in mouse spermatozoa. *Nutrients.* 2014; 6:489–503. [PubMed: 24473232]
- Morita Y, Wada-Hiraike O, Yano T, Shirane A, Hirano M, Hiraike H, Koyama S, Oishi H, Yoshino O, Miyamoto Y, Sone K, Oda K, Nakagawa S, Tsutsui K, Taketani Y. Resveratrol promotes expression of SIRT1 and StAR in rat ovarian granulosa cells: an implicative role of SIRT1 in the ovary. *Reprod Biol Endocrinol.* 2012a; 10:14. [PubMed: 22357324]
- Morita Y, Wada-Hiraike O, Yano T, Shirane A, Hirano M, Hiraike H, Koyama S, Oishi H, Yoshino O, Miyamoto Y, Sone K, Oda K, Nakagawa S, Tsutsui K, Taketani Y. Resveratrol promotes expression of SIRT1 and StAR in rat ovarian granulosa cells: an implicative role of SIRT1 in the ovary. *Reprod Biol Endocrinol.* 2012b; 10:14. [PubMed: 22357324]
- Nickens KP, Patierno SR, Ceryak S. Chromium genotoxicity: a double-edged sword. *Chem Biol Interact.* 2010; 188:276–288. [PubMed: 20430016]
- Ortega I, Duleba AJ. Ovarian actions of resveratrol. *Ann N Y Acad Sci.* 2015; 1348:86–96. [PubMed: 26315293]
- Ortega I, Villanueva JA, Wong DH, Cress AB, Sokalska A, Stanley SD, Duleba AJ. Resveratrol reduces steroidogenesis in rat ovarian theca-interstitial cells: the role of inhibition of AKT/PKB signaling pathway. *Endocrinology.* 2012a; 153:4019–4029. [PubMed: 22719052]

- Ortega I, Wong DH, Villanueva JA, Cress AB, Sokalska A, Stanley SD, Duleba AJ. Effects of resveratrol on growth and function of rat ovarian granulosa cells. *Fertil Steril.* 2012b; 98:1563–1573. [PubMed: 22959450]
- Ortega I, Villanueva JA, Wong DH, Cress AB, Sokalska A, Stanley SD, Duleba AJ. Resveratrol potentiates effects of simvastatin on inhibition of rat ovarian theca-interstitial cells steroidogenesis. *J Ovarian Res.* 2014; 7:21. [PubMed: 24524197]
- Osman P. Rate and course of atresia during follicular development in the adult cyclic rat. *J Reprod Fertil.* 1985; 73:261–270. [PubMed: 4038517]
- Raftogianis R, Creveling C, Weinshilboum R, Weisz J. Chapter 6: estrogen metabolism by conjugation. *JNCI Monographs.* 2000; 2000:113–124.
- Rao GT, Rao VVSG, Ranganathan K, Surinaidu L, Mahesh J, Ramesh G. Assessment of groundwater contamination from a hazardous dump site in Ranipet, Tamil Nadu, India. *Hydrogeol J.* 2011; 19:1587–1598.
- Rocha-Gonzalez HI, Ambriz-Tututi M, Granados-Soto V. Resveratrol: a natural compound with pharmacological potential in neurodegenerative diseases. *CNS Neurosci Ther.* 2008; 14:234–247. [PubMed: 18684235]
- Rubiolo JA, Mithieux G, Vega FV. Resveratrol protects primary rat hepatocytes against oxidative stress damage: activation of the Nrf2 transcription factor and augmented activities of antioxidant enzymes. *Eur J Pharmacol.* 2008; 591:66–72. [PubMed: 18616940]
- Schmittgen TD, Livak KJ. Analyzing real-time PCR data by the comparative CT method. *Nat Protoc.* 2008; 3:1101–1108. [PubMed: 18546601]
- Shimada T, Hayes CL, Yamazaki H, Amin S, Hecht SS, Guengerich FP, Sutter TR. Activation of chemically diverse procarcinogens by human cytochrome P-450 1B1. *Cancer Res.* 1996; 56:2979–2984. [PubMed: 8674051]
- Shin SM, Cho IJ, Kim SG. Resveratrol protects mitochondria against oxidative stress through AMP-activated protein kinase-mediated glycogen synthase kinase-3 β inhibition downstream of poly(ADP-ribose)polymerase-LKB1 pathway. *Mol Pharmacol.* 2009; 76:884–895. [PubMed: 19620254]
- Shin JA, Oh S, Ahn JH, Park EM. Estrogen receptor-mediated resveratrol actions on blood-brain barrier of ovariectomized mice. *Neurobiol Aging.* 2015; 36:993–1006. [PubMed: 25448605]
- Shmitova LA. Content of hexavalent chromium in the biological substrates of pregnant women and puerperae engaged in the manufacture of chromium compounds. *Gig Tr Prof Zabol.* 1980:33–35.
- Simsek Y, Gurocak S, Turkoz Y, Akpolat N, Celik O, Ozer A, Yilmaz E, Turhan U, Ozyalin F. Ameliorative effects of resveratrol on acute ovarian toxicity induced by total body irradiation in young adult rats. *J Pediatr Adolesc Gynecol.* 2012; 25:262–266. [PubMed: 22840937]
- Sivakumar KK, Stanley JA, Arosh JA, Pepling ME, Burghardt RC, Banu SK. Prenatal exposure to chromium induces early reproductive senescence by increasing germ cell apoptosis and advancing germ cell cyst breakdown in the F1 offspring. *Dev Biol.* 2014; 388:22–34. [PubMed: 24530425]
- Spink BC, Katz BH, Hussain MM, Pang S, Connor SP, Aldous KM, Gierthy JF, Spink DC. SULT1A1 catalyzes 2-methoxyestradiol sulfonation in MCF-7 breast cancer cells. *Carcinogenesis.* 2000; 21:1947–1957. [PubMed: 11062153]
- Stanley JA, Lee J, Nithy TK, Arosh JA, Burghardt RC, Banu SK. Chromium-VI arrests cell cycle and decreases granulosa cell proliferation by down-regulating cyclin-dependent kinases (CDK) and cyclins and up-regulating CDK-inhibitors. *Reprod Toxicol.* 2011; 32:112–123. [PubMed: 21621607]
- Stanley JA, Sivakumar KK, Nithy TK, Arosh JA, Hoyer PB, Burghardt RC, Banu SK. Postnatal exposure to chromium through mother's milk accelerates follicular atresia in F1 offspring through increased oxidative stress and depletion of antioxidant enzymes. *Free Radic Biol Med.* 2013; 61C: 179–196.
- Stanley JA, Sivakumar KK, Arosh JA, Burghardt RC, Banu SK. Edaravone mitigates hexavalent chromium-induced oxidative stress and depletion of antioxidant enzymes while estrogen restores antioxidant enzymes in the rat ovary in F1 offspring. *Biol Reprod.* 2014; 91:12. [PubMed: 24804965]

- Stanley JA, Arosh JA, Burghardt RC, Banu SK. A fetal whole ovarian culture model for the evaluation of CrVI-induced developmental toxicity during germ cell nest breakdown. *Toxicol Appl Pharmacol.* 2015; 289:58–69. [PubMed: 26348139]
- Supornsilchai V, Svechnikov K, Seidlova-Wuttke D, Wuttke W, Soder O. Phytoestrogen resveratrol suppresses steroidogenesis by rat adrenocortical cells by inhibiting cytochrome P450 c21-hydroxylase. *Horm Res.* 2005; 64:280–286. [PubMed: 16269870]
- Svechnikov K, Spatafora C, Svechnikova I, Tringali C, Soder O. Effects of resveratrol analogs on steroidogenesis and mitochondrial function in rat Leydig cells in vitro. *J Appl Toxicol.* 2009; 29:673–680. [PubMed: 19603415]
- Talalay P, Dinkova-Kostova AT, Holtzclaw WD. Importance of phase 2 gene regulation in protection against electrophile and reactive oxygen toxicity and carcinogenesis. *Adv Enzym Regul.* 2003; 43:121–134.
- Townsend DM, Tew KD, Tapiero H. The importance of glutathione in human disease. *Biomed Pharmacother.* 2003; 57:145–155. [PubMed: 12818476]
- Ungvari Z, Orosz Z, Rivera A, Labinskyy N, Xiangmin Z, Olson S, Podlutzky A, Csiszar A. Resveratrol increases vascular oxidative stress resistance. *Am J Physiol Heart Circ Physiol.* 2007; 292:H2417–H2424. [PubMed: 17220179]
- USEPA. US-Environmental-Protection-Agency. National primary drinking water regulations. 2009. p. 1-6. EPA 816-F-09-004
- Webster, IA. Hinkley Groundwater Remediation Project — IRP Manager Community Briefing No. 5. Project Navigator Ltd; 2012. p. 1-40.
- Yu, CW., Shin, YG., Chow, A., Li, YM., Kosmeder, JW., Lee, YS., Hirschelman, WH., Pezzuto, JM., Mehta, RG., van Breemen, RB. Human, Rat, and Mouse Metabolism of Resveratrol. 2002.
- Yu W, Fu YC, Wang W. Cellular and molecular effects of resveratrol in health and disease. *J Cell Biochem.* 2012; 113:752–759. [PubMed: 22065601]
- Zhang JD, Li XL. Chromium pollution of soil and water in Jinzhou. *Zhonghua yu fang yi xue za zhi [Chin J prev Med].* 1987; 21:262–264.
- Zhang Y, Liu Y, Wang T, Li B, Li H, Wang Z, Yang B. Resveratrol, a natural ingredient of grape skin: antiarrhythmic efficacy and ionic mechanisms. *Biochem Biophys Res Commun.* 2006; 340:1192–1199. [PubMed: 16406237]
- Zhao XY, Li GY, Liu Y, Chai LM, Chen JX, Zhang Y, Du ZM, Lu YJ, Yang BF. Resveratrol protects against arsenic trioxide-induced cardiotoxicity in vitro and in vivo. *Br J Pharmacol.* 2008; 154:105–113. [PubMed: 18332854]

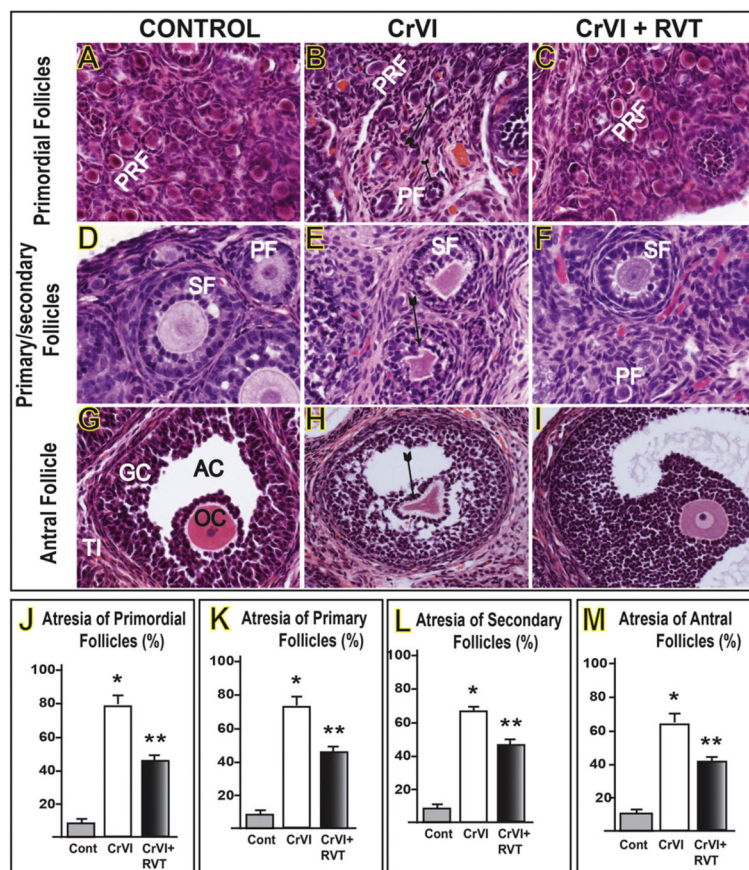


Fig. 1. Mitigative effects of RVT on CrVI-induced follicular atresia. Lactating dams ($n = 5$) received CrVI (50 ppm) in drinking water with or without RVT, as described in materials and methods. Suckling F1 female offspring ($n = 20$) received respective treatments through dam's milk during PND 1–21. On PND 25 ovaries were harvested, paraffin-embedded sections were stained with H&E, and atretic primordial, primary, secondary and antral follicle numbers were counted (J–M) in serial sections. Representative images of control primordial (A), primary or secondary (D) and antral (G) follicle; CrVI-treated primordial (B), primary or secondary (E) and antral (H) follicle; CrVI + RVT-treated primordial (C), primary or secondary (F) and antral (I) follicle are shown. Arrowheads in Figures A, B and C indicate primordial follicles. Arrowheads in Figures E and H indicate atretic secondary and antral follicles, respectively. The width of field for each image is 220 or 350 μm . PRM - Primordial follicle; PR - Primary follicle; SF - Secondary follicle; AC - antrum; OC - oocyte; GC - Granulosa cells; TI - Theca interstitial cells. Data are presented as the mean \pm SEM of 10 ovaries (2 ovaries/litter) from F1 rats. *Control vs CrVI; **CrVI vs CrVI + RVT, $P < 0.05$.

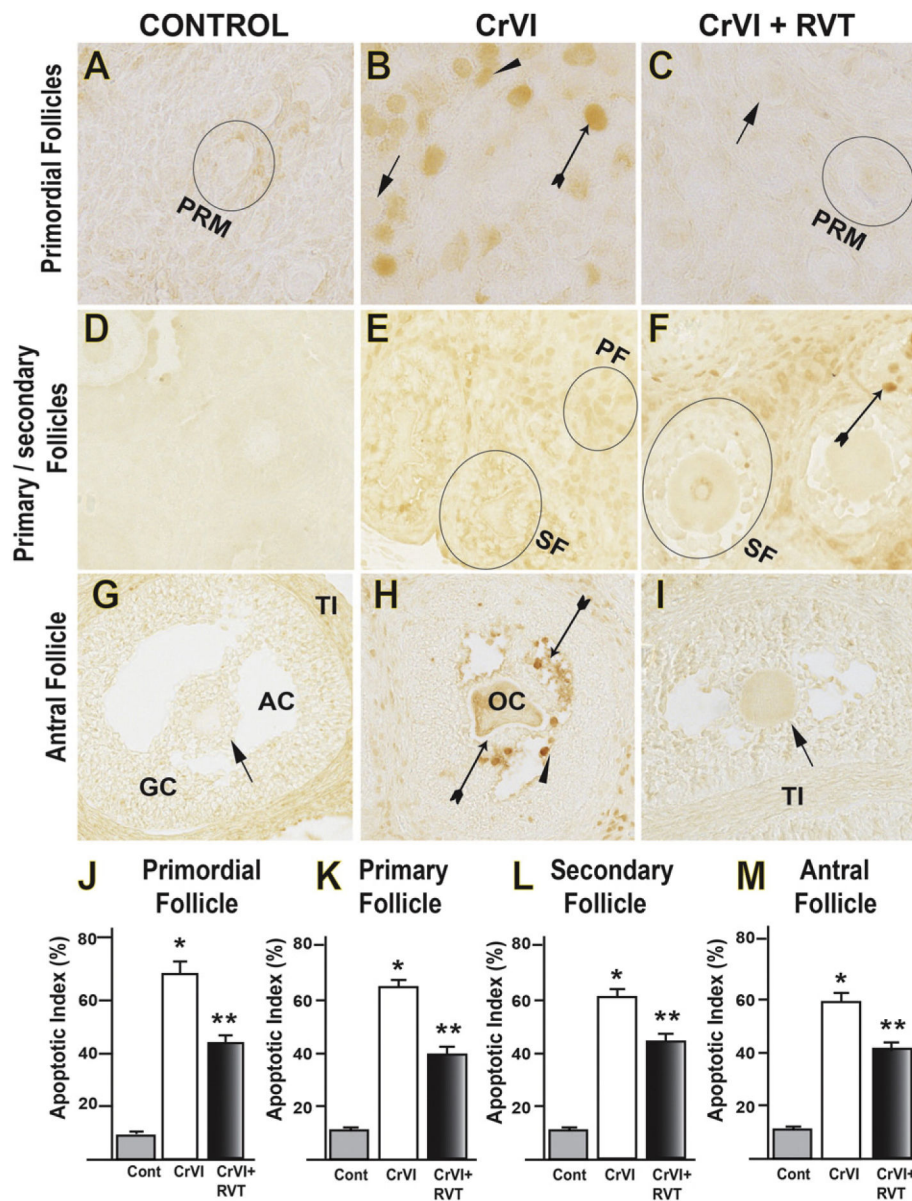


Fig. 2. Mitigative effects of RVT on CrVI-induced apoptosis. TUNEL assay was performed in paraffin-embedded sections of the ovary. Intensity of TUNEL staining was measured in oocytes (OC), and granulosa (GC) and theca (TI) cells as described. Representative images of control primordial (A), primary or secondary (D) and antral (G) follicle; CrVI-treated primordial (B), primary or secondary (E) and antral (H) follicle; CrVI + RVT-treated primordial (C), primary or secondary (F) and antral (I) follicles are shown. Apoptotic indices of primordial (J), primary (K), secondary (L) and antral (M) follicles are shown in histogram. The width of field for each image is 220 or 350 μm . Arrows indicate germ cells or oocytes; arrowheads indicate granulosa cells. Special arrows indicate apoptotic cells. PRM - Primordial follicle; PR - Primary follicle; SF - Secondary follicle; AC - antrum; OC - oocyte; GC - Granulosa cells; TI - Theca interstitial cells. Data are presented as the mean \pm

SEM of 10 ovaries (2 ovaries/litter) from F1 rats. *Control vs CrVI; **CrVI vs CrVI + RVT, $P < 0.05$.

Author Manuscript

Author Manuscript

Author Manuscript

Author Manuscript

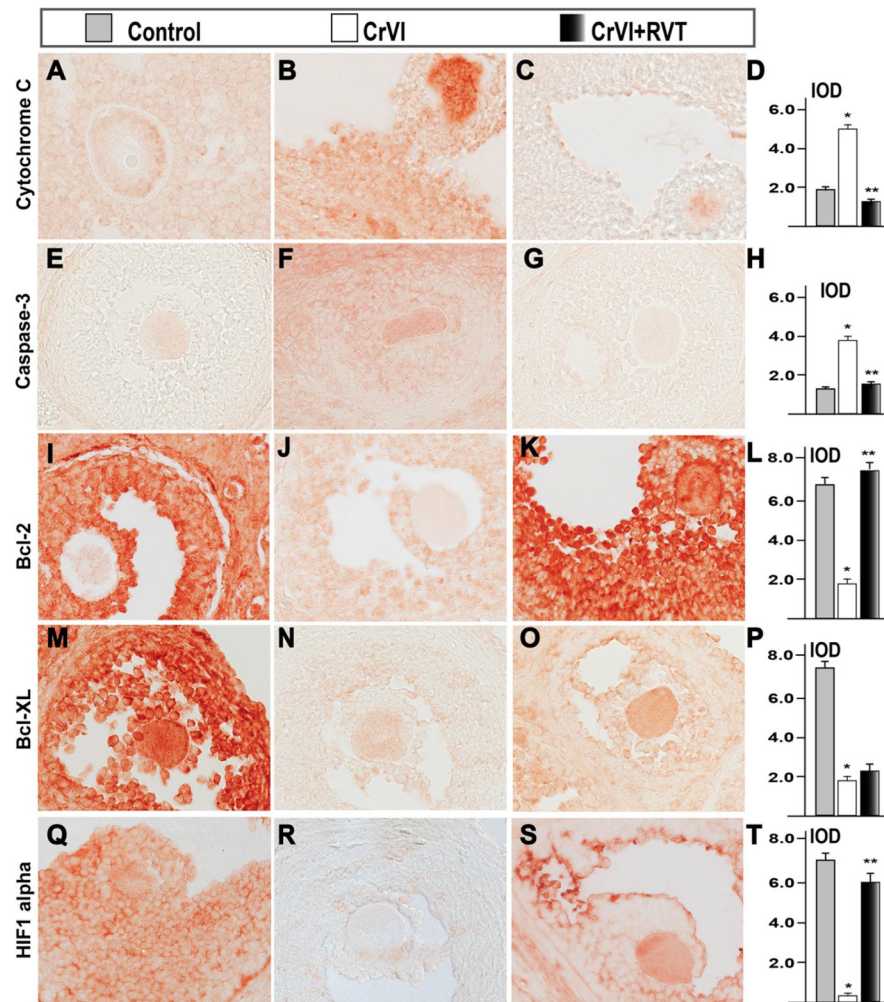


Fig. 3. Mitigative effects of RVT on CrVI-induced changes in cell survival and cell death proteins. Lactating dams ($n = 5$) received CrVI (50 ppm) in drinking water with or without RVT, as described in materials and methods. Suckling F1 female offspring ($n = 20$) received respective treatments through dam's milk during PND 1–21. On PND 25, ovaries were harvested from F1 rats and IHC was performed in paraffin-embedded tissue sections. Average of staining intensity (Integrated Optical Density, IOD) in oocytes and granulosa and theca cells was calculated. Representative images of cytochrome C: control (A), CrVI-50 ppm (B), CrVI + RVT (C), histogram of average IOD (D); caspase-3: control (E), CrVI-50 ppm (F), CrVI + RVT (G), histogram of average IOD (H); Bcl-2: control (I), CrVI-50 ppm (J), CrVI + RVT (K), histogram of average IOD (L); Bcl-XL: control (M), CrVI-50 ppm (N), CrVI + RVT (O), histogram of average IOD (P); HIF1 α : control (Q), CrVI-50 ppm (R), CrVI + RVT (S), histogram of average IOD (T) are shown. The width of field for each image is 220 or 350 μm . Data are presented as the mean \pm SEM of 10 ovaries (2 ovaries/litter) from F1 rats. *Control vs CrVI; **CrVI vs CrVI + RVT, $P < 0.05$.

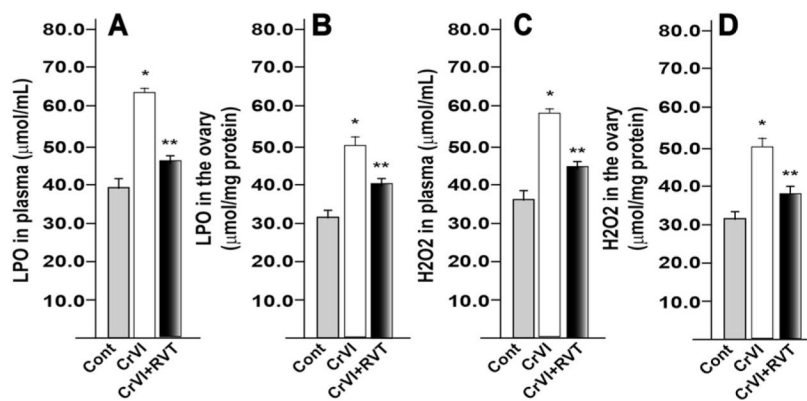


Fig. 4. Mitigative effects of RVT on CrVI-induced oxidative stress in the ovary and plasma. Lactating dams ($n = 5$) were exposed to CrVI (50 ppm) in drinking water with or without RVT treatment. Suckling F1 female offspring ($n = 20$) received respective treatments through dam's milk during PND 1–21. On PND 25, ovaries were harvested and levels of free radicals (LPO and H₂O₂) were estimated in the plasma (A & C) and homogenates (B & D) of the whole ovaries. Data are presented as the mean \pm SEM of 10 ovaries (2 ovaries/litter) from F1 rats. *Control vs CrVI; **CrVI vs CrVI + RVT, $P < 0.05$.

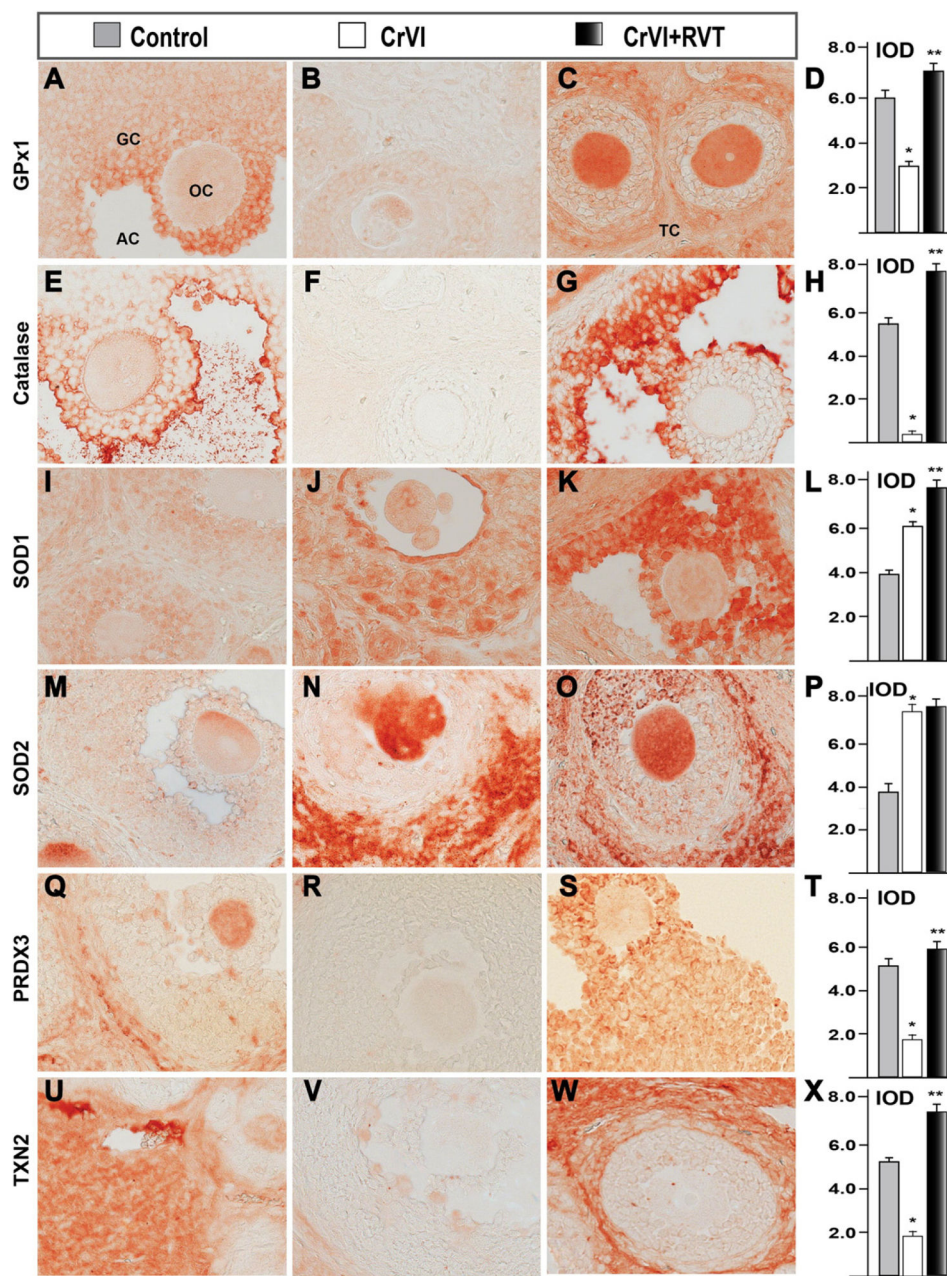


Fig. 5. Mitigative effects of RVT on CrVI-induced changes in antioxidant proteins. Lactating dams ($n = 5$) received CrVI (50 ppm) in drinking water with or without RVT, as described in materials and methods. Suckling F1 female offspring ($n = 20$) received respective treatments through dam's milk during PND 1–21. On PND 25, ovaries were harvested from F1 rats and IHC was performed in paraffin-embedded tissue sections. Average of staining intensity (Integrated Optical Density, IOD) in oocytes and granulosa and theca cells was calculated. Representative images of GPx1: control (A), CrVI-50 ppm (B), CrVI + RVT (C), histogram of average IOD (D); catalase: control (E), CrVI-50 ppm (F), CrVI + RVT (G), histogram of average IOD (H); SOD1: control (I), CrVI-50 ppm (J), CrVI + RVT (K), histogram of

average IOD (L); SOD2: control (M), CrVI-50 ppm (N), CrVI + RVT (O), histogram of average IOD (P); PRDX3: control (Q), CrVI-50 ppm (R), CrVI + RVT (S), histogram of average IOD (T); TXN2: control (U), CrVI-50 ppm (V), CrVI + RVT (W), histogram of average IOD (X) are shown. The width of field for each image is 220 or 350 μm . Data are presented as the mean \pm SEM of 10 ovaries (2 ovaries/litter) from F1 rats. *Control vs CrVI; **CrVI vs CrVI + RVT, $P < 0.05$.

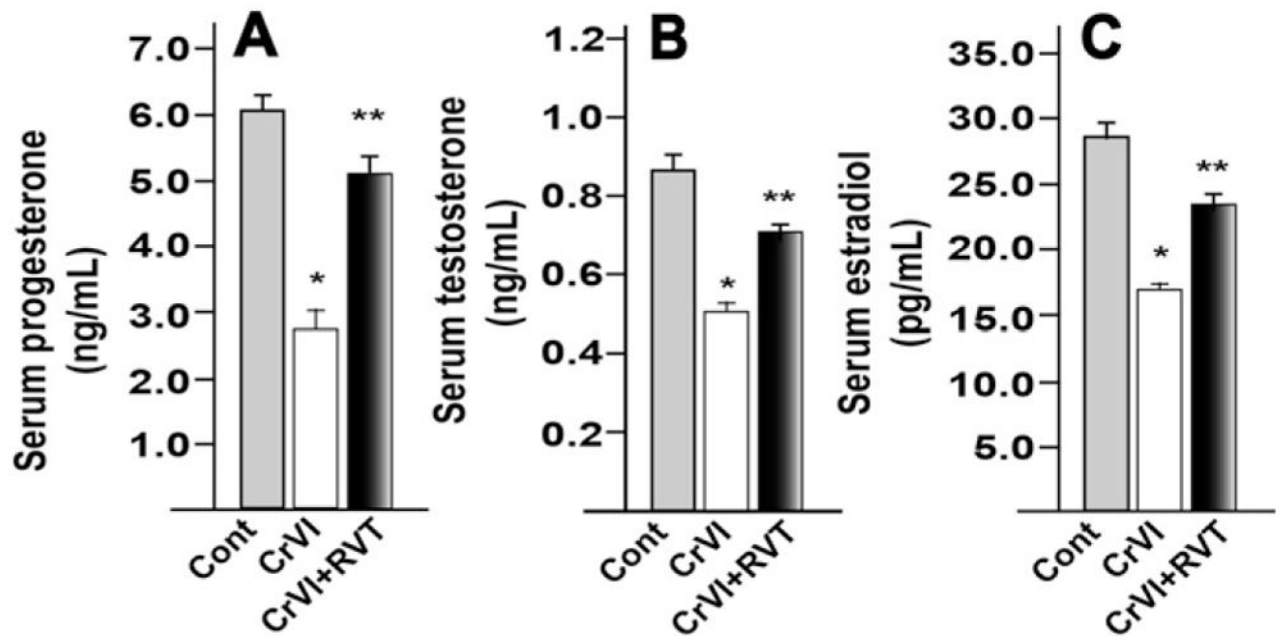


Fig. 6. Mitigative effects of RVT on CrVI-induced changes in progesterone (P4), testosterone (T), and estradiol (E₂). Lactating dams (n = 5) were exposed to CrVI (50 ppm) in drinking water with or without RVT treatment. Suckling F1 female offspring (n = 20) received respective treatments through dam's milk during PND 1–21. On PND 25, F1 females were euthanized, and P4 (A), T (B), and E₂ (C) in the serum were estimated. Data are presented as the mean ± SEM of 10 F1 rats (2 rats/litter). *Control vs CrVI; **CrVI vs CrVI + RVT, $P < 0.05$.

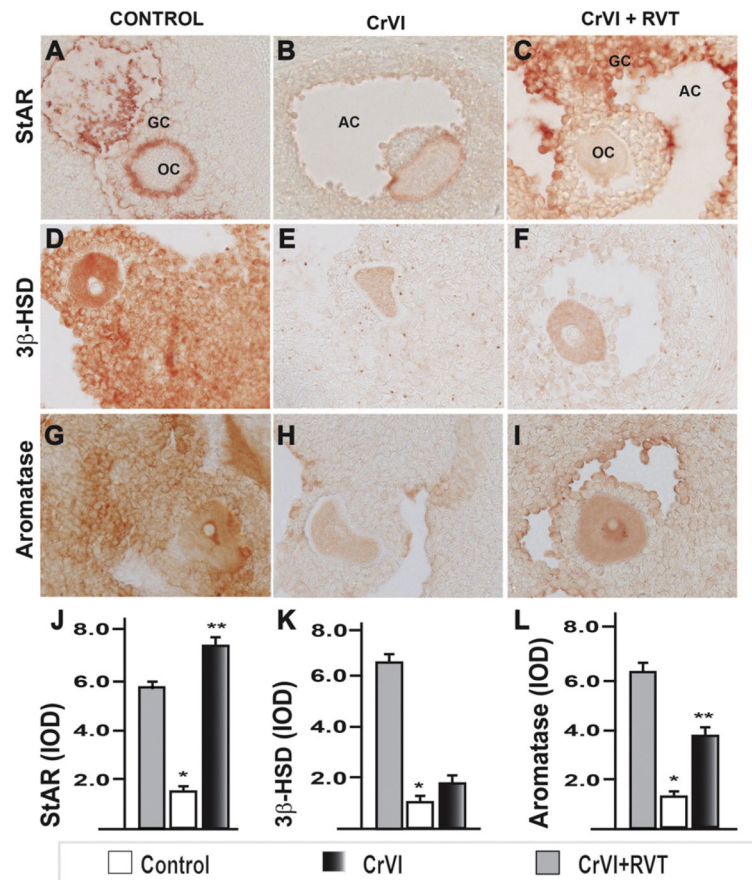


Fig. 7. Mitigative effects of RVT on CrVI-induced changes in StAR, 3βHSD and aromatase. Lactating dams (n = 5) received CrVI (50 ppm) in drinking water with or without RVT, as described in materials and methods. Suckling F1 female offspring (n = 20) received respective treatments through dam's milk during PND 1–21. On PND 25, ovaries were harvested from F1 rats and IHC was performed in paraffin-embedded tissue sections. Average of staining intensity (Integrated Optical Density, IOD) in oocytes and granulosa and theca cells was calculated. Representative images of StAR: control (A), CrVI-50 ppm (B), CrVI + RVT (C), histogram of average IOD (J); 3βHSD: control (D), CrVI-50 ppm (E), CrVI + RVT (F), histogram of average IOD (K); aromatase: control (G), CrVI-50 ppm (H), CrVI + RVT (I), histogram of average IOD (L) are shown. The width of field for each image is 220 or 350 μm. Data are presented as the mean ± SEM of 10 ovaries (2 ovaries/litter) from F1 rats. *Control vs CrVI; **CrVI vs CrVI + RVT, $P < 0.05$.

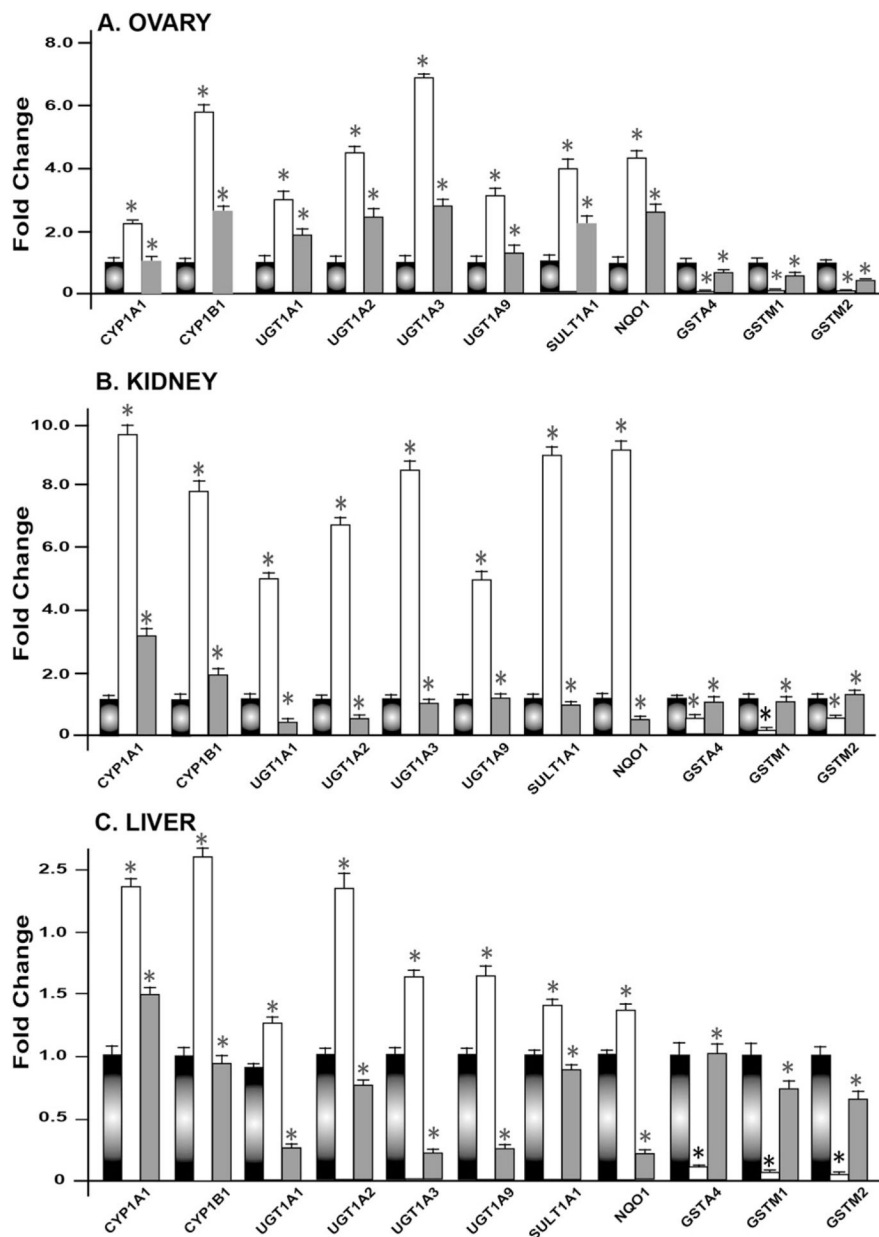


Fig. 8. Mitigative effects of RVT on CrVI-induced changes in the gene expression of E₂ metabolism in the ovary, kidney and liver. Lactating dams (n = 5) received CrVI (50 ppm) in drinking water with or without RVT, as described in materials and methods. Suckling F1 female offspring (n = 20) received respective treatments through dam’s milk during PND 1–21. On PND 25, ovaries, kidney and liver were harvested from F1 rats, mRNA isolated and real-time PCR was performed as described in materials and methods. Expression of *Cyp1a1*, *Cyp1b1*, *Ugt1a1*, *Ugt1a2*, *Ugt1a3*, *Ugt1a9*, *Sult1a1*, *Nqo1*, *Gstm1*, *Gstm2* and *Gsta4* in the ovary (A), kidney (B) and the liver (C). Data are presented as the mean ± SEM of 10 ovaries or kidney or liver (2 samples/litter) from F1 rats. *Control vs CrVI or CrVI + RVT, *P* < 0.05.

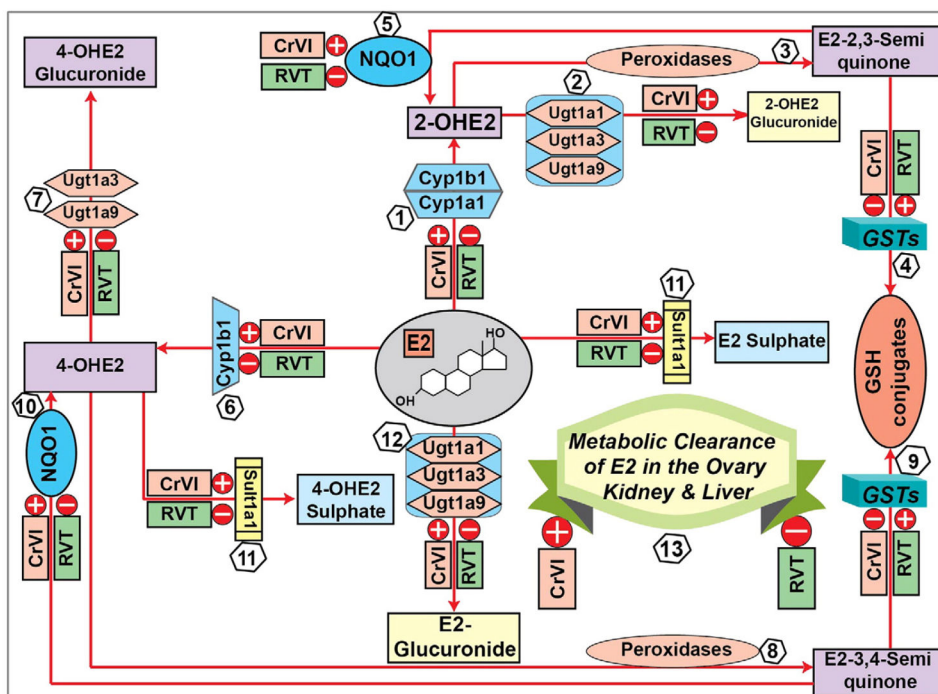


Fig. 9. Schematic diagram of regulation of E₂ metabolism by RVT against CrVI-toxicity. (1) Cyp1a1 and Cyp1b1 catalyze the conversion of E₂ into 2-OHE₂. (2) *Ugt1a1*, *Ugt1a3* and *Ugt1a9* catalyze the conversion of 2-OHE₂ into 2-OHE₂ glucuronide. (3) 2-OHE₂ is converted by peroxidases into E₂-2,3-semiquinone (E₂-2,3-semQ). (4) GSH-S-transferases (GSTs) convert E₂-2,3-semQ into GSH-E₂ conjugates. (5) Nqo1 catalyzes the conversion of E₂-2,3-semQ into 2-OHE₂. (6) Cyp1b1 catalyzes the conversion of E₂ into 4-OHE₂. (7) *Ugt1a3* and *Ugt1a9* catalyze the conversion of 4-OHE₂ into 4-OHE₂ glucuronide. (8) 4-OHE₂ is converted by peroxidases into E₂-3,4-semiquinones (E₂-3,4-semQ). (9) GSTs convert E₂-3,4-semQ into GSH-E₂ conjugates. (10) Nqo1 converts E₂-3,4-semQ into 4-OHE₂. (11) Sult1a1 converts 4-OHE₂ into 4-OHE₂ sulphate; and E₂ into E₂-sulphate. (12) *Ugt1a1*, *Ugt1a3* and *Ugt1a9* catalyze the conversion of E₂ into E₂-glucuronide. CrVI upregulated *Cyp1a1*, *Cyp1b1*, *Ugt1a1*, *Ugt1a3*, *Ugt1a9* and *Nqo1* which was mitigated by RVT. CrVI down regulated *Gstm1*, *Gstm2* and *Gsta4* which was mitigated by RVT. (13) Taken together, CrVI increased the metabolic clearance of E₂ in the ovary, kidney and liver and decreased E₂ levels in the blood; and RVT mitigated the effects of CrVI, delayed the clearance of E₂ from the blood by modulating the transcription of genes involved in E₂ metabolism.

Table 1

Antibody table (source, catalog numbers, dilutions, host species and antigen sequences).

S-no	Peptide/protein target	Antigen sequence	Name of antibody	Manufacturer; catalog #	Species raised in	Dilution used
1	Cytochrome C	Synthetic peptide conjugated to KLH derived from within residues 50 to the C-terminus of human cytochrome c	Rabbit anti-cytochrome c	Abcam; ab90529	Rabbit polyclonal	1:2000
2	Cleaved-caspase-3	Synthetic peptide corresponding to amino-terminal residues adjacent to (Asp175) in human caspase-3	Rabbit anti-cleaved-caspase-3	Cell Signaling; 9661	Rabbit polyclonal	1:100
3	BCL2	N terminal amino acids 1–18 of Human Bcl-2; AGRTGYDNREIVMKYIHY	Rabbit anti-Bcl-2	Abcam; ab7973	Rabbit polyclonal	1:300
4	BCL-XL	Synthetic peptide corresponding to residues surrounding Asp61 of human Bcl-xL	Rabbit anti-BCL-xl	Cell Signaling; 2762	Rabbit polyclonal	1:25
5	HIF-1 α	Recombinant fragment corresponding to Human HIF-1- α aa 329–530	Mouse anti-HIF-1 α	Abcam; ab8366	Mouse monoclonal	1:1000
6	GPx1	Synthetic peptide (the amino acid sequence is considered to be commercially sensitive) (internal sequence)	Rabbit anti-GPX-1	Abcam; ab108427	Rabbit monoclonal	1:50
7	Catalase	Rat liver mitochondria	Mouse anti-catalase	Mitosciences; MS721-SP	Mouse monoclonal	1:700
8	SOD1	Synthetic peptide corresponding to residues near the amino-terminus of human SOD1	Rabbit anti-SOD1	Cell Signaling; 2770	Rabbit polyclonal	1:25
9	SOD2	Full length protein (human)	Rabbit anti-SOD-2	Abcam; ab13533	Rabbit polyclonal	1:200
10	PRDX3	Synthetic peptide conjugated to KLH derived from within residues 200 to the C-terminus of Human Peroxiredoxin 3	Rabbit anti-PRDX3	Abcam; ab73349	Rabbit polyclonal	1:100
11	TXN2	Recombinant full length protein (human)	Mouse anti-TXN2	Abcam; ab16857	Mouse monoclonal	1:200
12	SiAR	Synthetic peptide within Human SiAR aa 130–180 conjugated to Keyhole Limpet Haemocyanin (KLH).	Rabbit anti-SiAR	Abcam; ab203193	Rabbit polyclonal	1:200
13	3 β -HSD	Synthetic peptide (the amino acid sequence is considered to be commercially sensitive)	Rabbit anti-HSD3B1	Abcam; ab150384	Rabbit monoclonal	1:200
14	CYP19/aromatase	Synthetic peptide from human cytochrome P450 19A1 (aa221–270)	Rabbit anti-CYP19/aromatase	LS Bio; LS: C119485	Rabbit polyclonal	1:100

Table 2

Oligonucleotide primers.

<i>CYP1A1_Forward</i>	5'-TAA TCA AAG AGC ACT ACA GGA C -3'
<i>CYP1A1_Reverse</i>	5'- TGG ATC TTT CTC TGT ATC CTA G -3'
<i>CYP1B1_Forward</i>	5'- GCT CAT CCT CTT TAC CAG ATA C -3'
<i>CYP1B1_Reverse</i>	5'- ATC AAA GTC CTC TGG GTT AGA C -3'
<i>UGT1A1_Forward</i>	5'- CTG CTG TGT ACT TCT TGA ATG C -3'
<i>UGT1A1_Reverse</i>	5'- GGG TAA TCT TTC ACA AAG TCG T -3'
<i>UGT1A2_Forward</i>	5'- ATC TCT ACG CAA ATT CTT GTG C -3'
<i>UGT1A2_Reverse</i>	5'- GAG TAG GTT CGG AAT ATA AGA G -3'
<i>UGT1A3_Forward</i>	5'- CAT ACA CCA AGG AAG AGT ACA G -3'
<i>UGT1A3_Reverse</i>	5'- TAT TCT TCA CTC TGT CTA GGA AGC -3'
<i>UGT1A9_Forward</i>	5'- ATA CTC AAT TCC TTA CAC TGT G -3'
<i>UGT1A9_Reverse</i>	5'- GTC TAG GAA CAT AAG AAG GAA G -3'
<i>SULT1A1_Forward</i>	5'- GTC TTG AAA CTT TGG AAG AGA C -3'
<i>SULT1A1_Reverse</i>	5'- CAT AGA AGA GAT AGA GAA CAG G -3'
<i>NQO1_Forward</i>	5'- AGG CTC TGA AGA AGA AAG GAT G -3'
<i>NQO1_Reverse</i>	5'- GTC TTC TTA TTC TGG AAA GGA C -3'
<i>GSTA4_Forward</i>	5'- GAG CCT AGC TTT AGC AGT GAA GAG -3'
<i>GSTA4_Reverse</i>	5'- AGA GCT CTA TCT TGC CTC TGG AAT G -3'
<i>GSTM1_Forward</i>	5'- CGC CTG CTC CTG GAA TAC ACA GA -3'
<i>GSTM1_Reverse</i>	5'- CAG GAA CTC AGA GTA GAG CTT CAT C -3'
<i>GSTM2_Forward</i>	5'- GAC ACT GGG TTA CTG GGA CAT CCG -3'
<i>GSTM2_Reverse</i>	5'- CTC AGG GAG ACC CTC TAA GTA CTC -3'
<i>β-Actin_Forward</i>	5'- CAA CCT TCT TGC AGC TCC TC -3'
<i>β-Actin_Reverse</i>	5'- TTC TGA CCC ATA CCC ACC AT -3'